

Electronic supplementary information

Introducing redox-active ferrocenyl moiety onto polythiophene derivative towards high-performance flexible all-solid-state symmetric supercapacitor

Bulin Chen,^{ab} Wai-Yeung Wong^{*ab}

^a Department of Applied Biology and Chemical Technology and Research Institute for Smart Energy, The Hong Kong Polytechnic University, Hung Hom, Hong Kong, P. R. China.

^b The Hong Kong Polytechnic University Shenzhen Research Institute, Shenzhen 518057, P. R. China.

* Corresponding author. E-mail: wai-yeung.wong@polyu.edu.hk.

Table of Content

1. Chemicals and materials	2
2. Physical characterizations	2
3. Electrochemical characterizations and measurements	2
Fig. S1	4
Fig. S2	4
Fig. S3	5
Fig. S4	6
Table S1	7
Table S2	8
References	9

1. Chemicals and materials

All reagents and chemicals, unless specified, were purchased from commercial sources and used without further purification. All reactions were carried out under a nitrogen atmosphere by using standard Schlenk techniques. Solvents for the synthesis were dried and distilled from appropriate drying agents under an inert atmosphere prior to use, and solvents used in the electrochemical workstation were bubbled with nitrogen at room temperature for one hour before use. Glassy carbon working electrode (CHI104, the diameter of the round conductive area is measured as 0.3 cm), Ag/AgCl (3 M KCl) reference electrode (CHI111), Ag/Ag⁺ reference electrode (CHI112), and platinum wire counter electrode (CHI115) were all purchased from Chenhua Instrumental Co., Ltd., Shanghai, China. Carbon cloths and carbon paper were purchased from CeTech Co., Ltd., Taiwan, China and Toray Industries, Inc., respectively, and tailored into desirable sizes before use.

2. Physical characterizations

All synthesized compounds were characterized by nuclear magnetic resonance spectra on a Bruker Advance-III 400 MHz Fourier Transform NMR System at room temperature. The ¹H NMR (400 MHz) and ¹³C NMR (100 MHz) spectra were referenced according to the tetramethylsilane internal standard. High-resolution mass spectrometry data were recorded on an Agilent 6540 Liquid Chromatography-Electrospray Ionization Quadrupole-Time-of-flight Mass Spectrometer. XRD patterns were recorded by Rigaku SmartLab 9kW-Advance X-ray Diffractometer. SEM images and EDS data were obtained from Tescan VEGA3 Scanning Electron Microscope. XPS patterns were recorded at Thermo Scientific Nexsa G2 X-Ray Photoelectron Spectrometer System.

3. Electrochemical characterizations and measurements

All electrochemical characterizations (GCD, CV and EIS) were performed on a Chenhua CHI660E electrochemical workstation at room temperature. Experiments to determine the electrochemical properties and capacitive performances of the as-prepared electrodes were performed in a three-electrode system in aqueous electrolytes (1 M H₂SO₄, 1 M Na₂SO₄ or 1 M KOH), with a Ag/AgCl (3 M KCl) or Ag/Ag⁺ electrode and a platinum wire electrode serving as reference and counter electrodes, respectively. The performances of the devices were studied in a two-electrode system, with two identical electrodes serving as the positive and negative electrode, respectively. The GCD tests at specific current densities (1–32 mA cm⁻²) were realized via chronopotentiometry technology, with constant cathodic and anodic current values (A) set as the calculated results by the

known area (cm^{-2}) for each electrode and device. The Nyquist plots for the impedance study were collected in the frequency range from 10^{-2} to 10^6 Hz, with AC voltages of 5 mV amplitude referring to the open circuit potentials. Current density (I_a , mA cm^{-2}), areal specific capacitance (C_a , F cm^{-2}), Coulombic efficiency (η , %), energy density (E , Wh cm^{-2}) and power density (P , W cm^{-2}) in this paper

$$I_a = \frac{I}{A \times 1000}$$

$$C_a = \frac{I_a \times t_{\text{discharge}}}{V_{\text{max}} - V_{\text{min}}} \times 1000$$

$$\eta = \frac{t_{\text{discharge}}}{t_{\text{charge}}} \times 100$$

$$E = \frac{C_a \times (V_{\text{max}} - V_{\text{min}})^2}{2 \times 3600}$$

$$P = \frac{3600 \times E}{t_{\text{discharge}}}$$

were calculated by the equations below:

In the equations above, V_{max} (V), V_{min} (V) and I (A) are the high voltage, low voltage and constant current, respectively, all of which are the instrument settings of the GCD chronopotentiometry technology prior to the experiments; A (cm^2) is the area of the working electrodes or devices. $t_{\text{discharge}}$ and t_{charge} are the time periods (s) of charge and discharge processes read from the GCD curves, respectively.

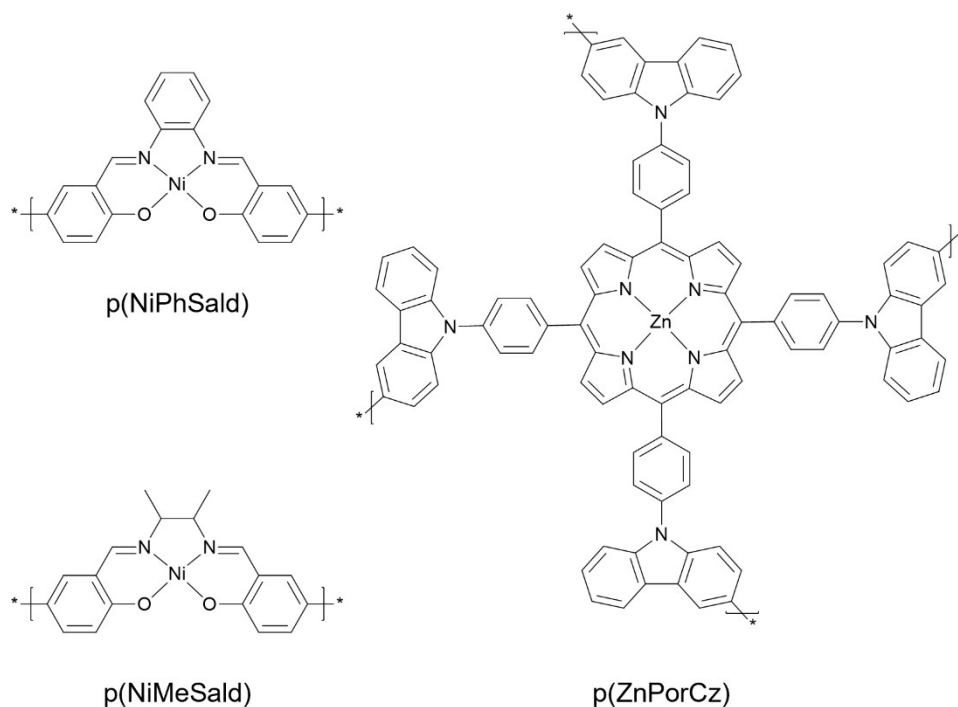


Fig. S1

Three reported conductive metallopolymers as SC electrode materials.¹⁻³

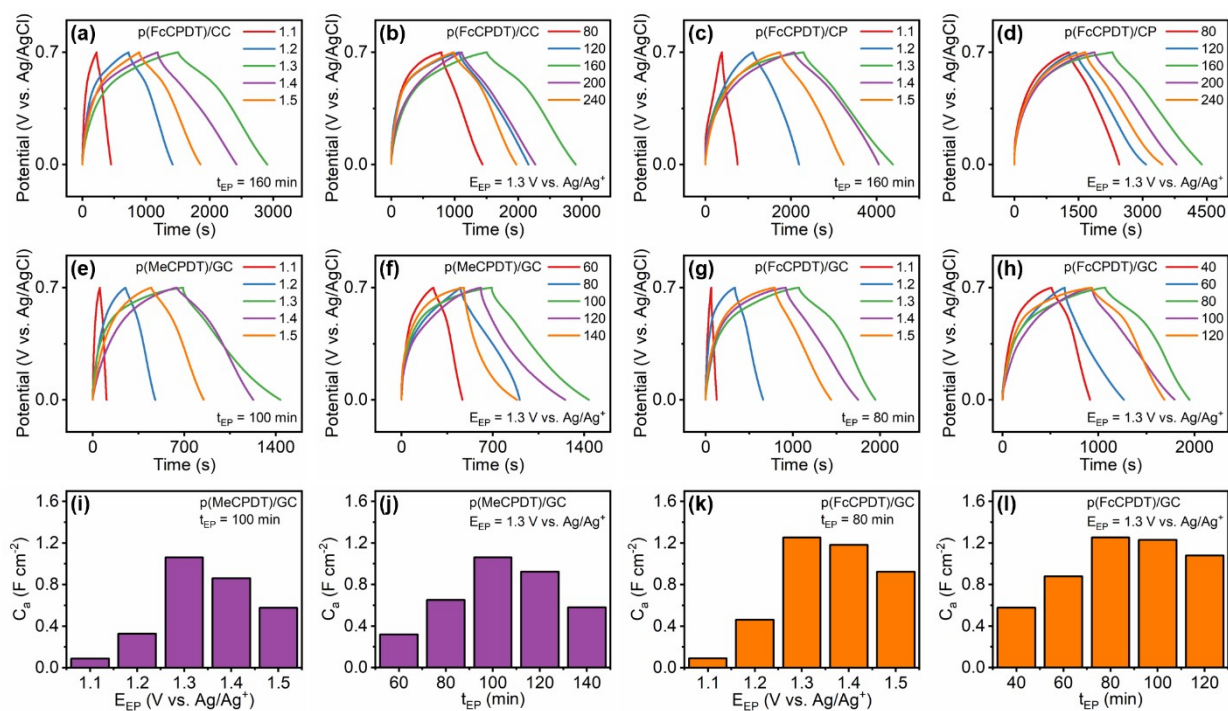


Fig. S2

(a-h) GCD curves and (i-j) as-calculated C_a values of the electrodes which were prepared via electropolymerization under different conditions in 1 M H₂SO₄ at the current density of 1 mA cm⁻².

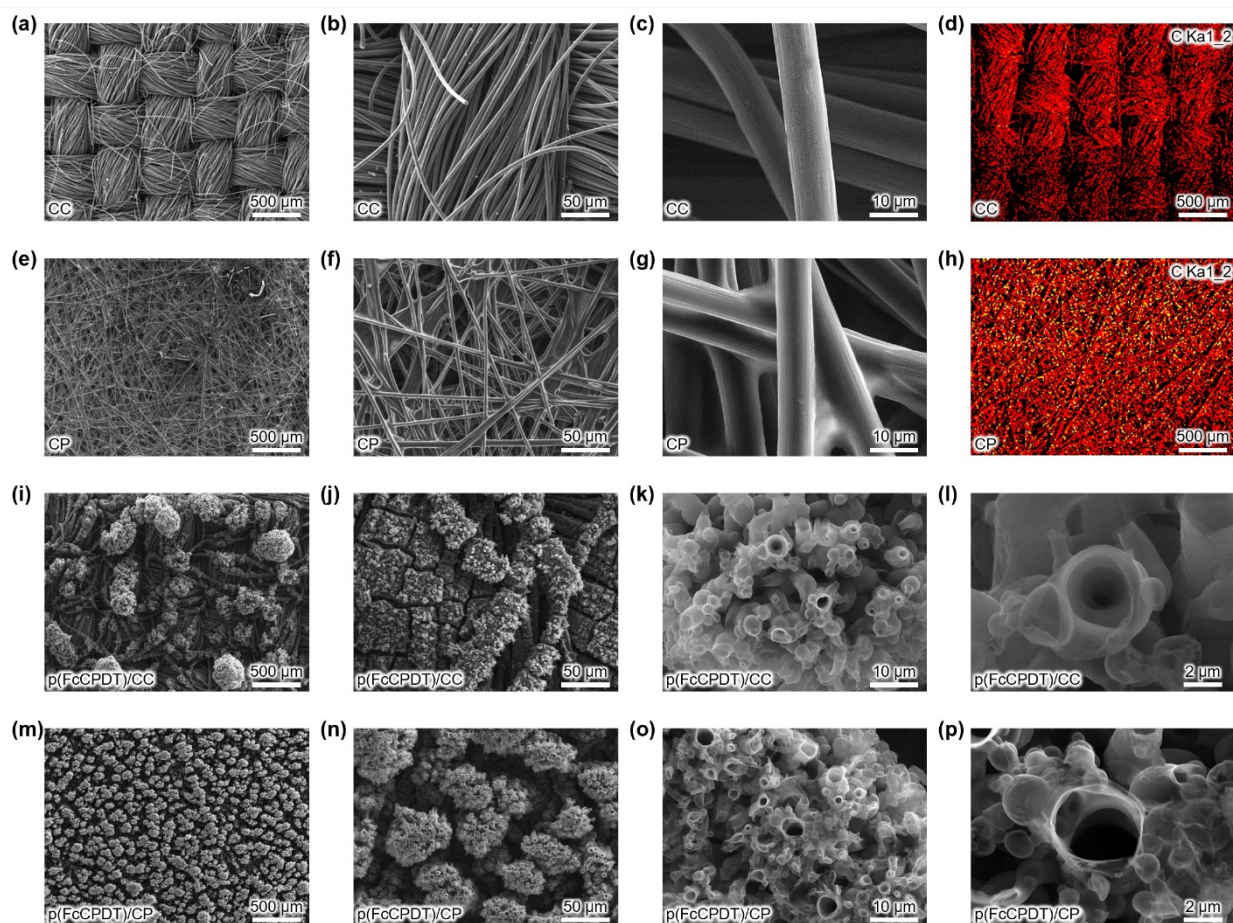


Fig. S3

SEM images of (a–c) CC, (e–g) CP, (i–l) optimized p(FcCPDT)/CC and (m–p) optimized p(FcCPDT)/CP. EDS elemental mapping of C for (d) CC and (h) CP.

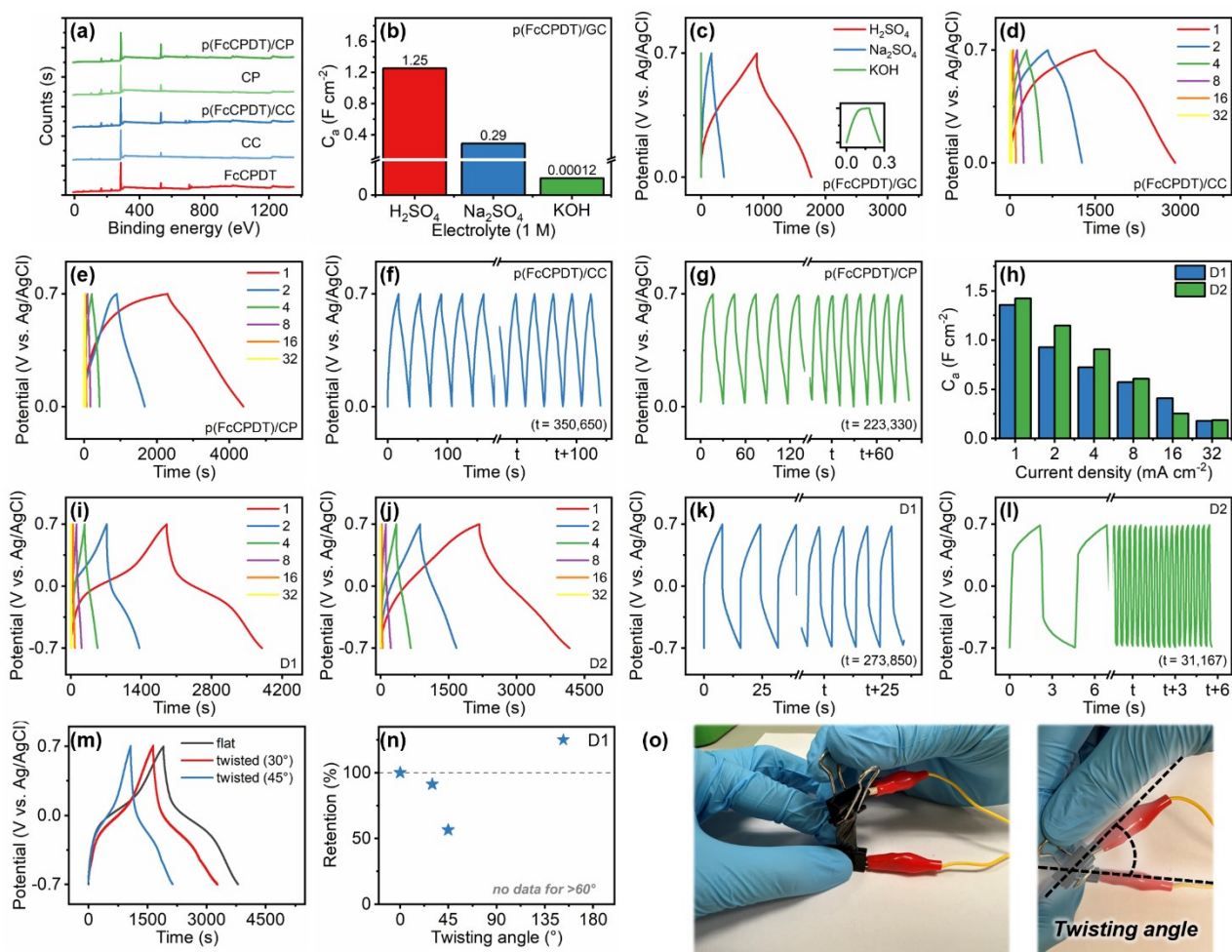


Fig. S4

(a) Full-spectra XPS patterns of the metallopolymer-coated electrodes in comparison with the corresponding monomer and EP substrates. (b) C_a and (c) GCD curves of the optimized p(FcCPDT)/GC at the current density of 1 mA cm⁻² in different aqueous electrolytes (1 M). GCD curves of the optimized (d) p(FcCPDT)/CC and (e) p(FcCPDT)/CP at various current densities in 1 M H₂SO₄. GCD curves of the optimized (f) p(FcCPDT)/CC and (g) p(FcCPDT)/CP during 10000 charge-discharge cycles at 32 mA cm⁻². (h) C_a of the devices D1 and D2 at different current densities. GCD curves of (i) D1 and (j) D2 at different current densities. GCD curves of (k) D1 and (l) D2 during 20000 and 15000 charge-discharge cycles at 32 mA cm⁻², respectively. (m) GCD curves and (n) C_a of D1 at different twisting states. (o) Digital photo images of twisted D1.

Table S1

Performance data of flexible and binder-free SC electrodes: the optimized p(FcCPDT)/CC and p(FcCPDT)/CP in comparison with those reported in the literature.

Electrode	C_a /(F cm ⁻²) ^a	Cycling stability ^{a, b}	Reference
p(FcCPDT)/CP	2.97 F cm ⁻² @ 1 mA cm ⁻²	86% @ 32 mA cm ⁻² (10,000)	this work
p(FcCPDT)/CC	2.00 F cm ⁻² @ 1 mA cm ⁻²	67% @ 32 mA cm ⁻² (10,000)	this work
PANI/MOF/CC	1.71 F cm ⁻² @ 0.4 mA cm ⁻²	60% @ 20 mA cm ⁻² (5,000)	4
MXene/MOF	1.64 F cm ⁻² @ 1 mA cm ⁻²	n/a	5
PEDOT/rGO	0.57 F cm ⁻² @ 0.5 mA cm ⁻²	97% @ 50 mA cm ⁻² (5,000)	6
Copolymer	0.43 F cm ⁻² @ 1 mA cm ⁻²	70% @ 2 mA cm ⁻² (1,000)	7
MOF/PPy	0.07 F cm ⁻² @ 0.2 mA cm ⁻²	100% @ 2 mA cm ⁻² (20,000)	8

^a What follows “@” is the current density.

^b The number in the bracket is the cycle number.

Abbreviations: PANI, polyaniline; MXene, transition metal carbides, carbonitrides or nitrides; PEDOT, poly(3,4-ethylenedioxythiophene); rGO, reduced graphene oxide; PPy, polypyrrole.

Table S2

Performance data of flexible ASS SC devices of sandwich configuration.

Electrode	C_a ^a	Maximum E	Maximum P	Cycling stability ^{a,b}	Reference
p(FcCPDT)/CC	1354 mF cm ⁻² @ 1 mA cm ⁻²	0.37 mW h cm ⁻²	22.4 mW cm ⁻²	88% @ 32 mA cm ⁻² (15,000)	This work, D1
Cotton fabric/PPy	669 mF cm ⁻² @ 0.2 mA cm ⁻²	81.7 μW h cm ⁻²	0.8 mW cm ⁻²	95.3% @ 4 mA cm ⁻² (10,000)	9
Cladophora nanocellulose paper/PEDOT	920 mF cm ⁻² @ 10 mA cm ⁻²	n/a	n/a	93% @ 30 mA cm ⁻² (15,000)	10
PEDOT:PSS/PVA/PMA A hydrogels	7.38 mF cm ⁻² @ 10 mV s ⁻¹	0.65 μW h cm ⁻²	0.17 mW cm ⁻²	82% @ 10 mV s ⁻¹ (2,000)	11
CC modified by sodium lignosulfonate/PANI hydrogel	1223 mF cm ⁻² @ 2 mA cm ⁻²	0.17 mW h cm ⁻²	10 mW cm ⁻²	84% @ 20 mA cm ⁻² (5,000)	12
PVA/PANI hydrogel	306 mF cm ⁻² @ 0.25 A g ⁻¹	n/a	n/a	86% @ 20 A g ⁻¹ (1,000)	13
PVA/PANI hydrogel	420 mF cm ⁻² @ 0.25 A g ⁻¹	n/a	n/a	100% @ 20 A g ⁻¹ (1,000)	14
Chitosan-derived carbon sheet/microfibrillated cellulose fiber film coated with PANI	3488.3 mF cm ⁻² @ 1 mA cm ⁻²	0.155 mW h cm ⁻²	20.02 mW cm ⁻²	90.1% @ 20 mA cm ⁻² (2,500)	15
Ti foil/TiO ₂ /MnO ₂ /PPy	122.5 mF cm ⁻² @ 1 mA cm ⁻²	n/a	n/a	94.1% @ 3 A g ⁻¹ (10,000)	16
Active carbon fiber cloth/PANI/CNTs/MnO ₂	2606 mF cm ⁻² @ 5 mA cm ⁻²	0.157 mW h cm ⁻²	10.37 mW cm ⁻²	82% @ 4 mA cm ⁻² (3,000)	17
Carbon fiber cloth/PANI/Ni-Mo-P	1072.5 mF cm ⁻² @ 0.5 mA cm ⁻²	0.38 mW h cm ⁻²	n/a	92.3% @ 40 mA cm ⁻² (2,000)	18

^a What follows “@” is either the current density or scan rate.^b The number in the bracket is the cycle number.

Abbreviations: PSS, polystyrene sulfonate; PMAA, poly(methacrylic acid); CNT, carbon nanotube.

References

1. C. Chen, Z. Zhu, X. Li and J. Li, *J. Appl. Polym. Sci.*, 2017, **134**.
2. H. Zhang, Y. Zhang, C. Gu and Y. Ma, *Adv. Energy Mater.*, 2015, **5**, 1402175.
3. K. Łepicka, P. Pieta, R. Gupta, M. Dabrowski and W. Kutner, *Electrochim. Acta*, 2018, **268**, 111-120.
4. J. Zhou, Y. Yuan, J. Tang and W. Tang, *Energy Storage Mater.*, 2019, **23**, 594-601.
5. W. Zhao, J. Peng, W. Wang, B. Jin, T. Chen, S. Liu, Q. Zhao and W. Huang, *Small*, 2019, **15**, 1901351.
6. Y. Li, Z. Xia, Q. Gong, X. Liu, Y. Yang, C. Chen and C. Qian, *Synth. Met.*, 2021, **280**, 116891.
7. A. Ringk, A. Lignie, Y. Hou, H. N. Alshareef and P. M. Beaujuge, *ACS Appl. Mater. Interfaces*, 2016, **8**, 12091-12100.
8. W. Zhao, W. Wang, J. Peng, T. Chen, B. Jin, S. Liu, W. Huang and Q. Zhao, *Dalton Trans.*, 2019, **48**, 9631-9638.
9. D. Sun, Q. Liu, C. Yi, J. Chen, D. Wang, Y. Wang, X. Liu, M. Li, K. Liu, P. Zhou and G. Sun, *Electrochim. Acta*, 2020, **354**, 136746.
10. Z. Wang, P. Tammela, J. Huo, P. Zhang, M. Strømme and L. Nyholm, *J. Mater. Chem. A*, 2016, **4**, 1714-1722.
11. C.-C. Shih, Y.-C. Lin, M. Gao, M. Wu, H.-C. Hsieh, N.-L. Wu and W.-C. Chen, *J. Power Sources*, 2019, **426**, 205-215.
12. D. Wu and W. Zhong, *J. Mater. Chem. A*, 2019, **7**, 5819-5830.
13. W. Li, F. Gao, X. Wang, N. Zhang and M. Ma, *Angew. Chem. Int. Ed.*, 2016, **55**, 9196-9201.
14. W. Li, H. Lu, N. Zhang and M. Ma, *ACS Appl. Mater. Interfaces*, 2017, **9**, 20142-20149.
15. Y. Zou, R. Liu, W. Zhong and W. Yang, *J. Mater. Chem. A*, 2018, **6**, 8568-8578.
16. Q. Zhu, K. Liu, J. Zhou, H. Hu, W. Chen and Y. Yu, *Chem. Eng. J.*, 2017, **321**, 554-563.
17. J. Wang, L. Dong, C. Xu, D. Ren, X. Ma and F. Kang, *ACS Appl. Mater. Interfaces*, 2018, **10**, 10851-10859.
18. L. Zhao, C. Yang, P. Shen, Z. Wang, C. Deng, L. Yang, J. Li and D. Qian, *Electrochim. Acta*, 2017, **249**, 318-327.